



ISSN 0975-413X
CODEN (USA): PCHHAX

Der Pharma Chemica, 2017, 9(14):164-177
(<http://www.derpharmachemica.com/archive.html>)

Thermal Kinetics Study of 4-((naphthalen-1-ylmethylene)amino)-benzene Sulfonamide Using TG/DTG Techniques

Venkatesan J¹, Sekar M^{1*}, Thanikachalam V², Manikandan G²

¹Department of Chemistry, PG and Research, Government Arts College, C. Mutlur, Chidambaram-608102, India

²Department of Chemistry, Annamalai University, Annamalainagar-608002, India

ABSTRACT

4-((Naphthalen-1-ylmethylene)-amino)-benzene Sulfonamide (NMABS) was synthesized with α -naphthaldehyde and 4-aminobenzenesulfonamide by condensation method and characterized by microanalysis, Fourier Transform Infrared (FT-IR) and Nuclear Magnetic Resonance (NMR) (¹H and ¹³C) techniques. Thermal decomposition of NMABS was studied by Thermogravimetric Analysis/Difference Thermo Gravimetry (TG/DTG) under dynamic oxygen atmosphere at different heating rates of 10, 15 and 20 K/min⁻¹ and decomposed into two steps as evidenced from the DTG curve. The model-free (Friedman, Kissinger-Akahira-Sunose (KAS) and Flynn-Wall-Ozawa (FWO)) and model-fitting methods (Coats-Redfern (CR)) were used to analyze non-isothermal solid-state kinetic data. Invariant kinetic parameters are consistent with the average values obtained by Friedman and KAS isoconversional methods. Each decomposition step is followed in different kinetic models, the thermal decomposition of NMABS was described by a second-order type reaction ($g(\alpha)=(1-\alpha)^{-1}-1$ (stage 1)) and 3-D Diffusion-Jander equation ($g(\alpha)=[1-(1-\alpha)^{1/3}]^2$ (stage 2)). The positive values of ΔH^\ddagger and ΔG^\ddagger indicate that the decomposition process is absorption of heat and non-spontaneous nature.

Keywords: Sulfonamide Schiff's bases, Thermal decomposition, Solid state kinetics, Invariant kinetic parameters, Thermodynamic parameters

INTRODUCTION

Sulfonamides and its derivatives are used as antimicrobial agents [1-4], *in vitro* antitumor activity [5] and cytotoxicity bioassay [6-8], hemolysis assay naphthyl appended sulphonamide Schiff bases and drug must reach the target receptor and its journey (pharmacodynamics) is associated with the Absorption, Distribution, Metabolism and Excretion (ADME) [9], biological activity towards *Colletotrichum gloeosporioides* spores germination activity [10], antioxidant activities [11], anti-inflammatory activity [12], introduce an acid-base indicator that derived from a pharmaceutical active material [13], bio-assay were tested against important antibacterial and antifungal activity [14-16].

The offering Quantitative Structure Activity Relationship (QSAR) model is very easy to computation and physico-chemically interpretable. Sensitivity analysis was used to determine the relative importance of each descriptor in Artificial Neural Network (ANN) model. The order of importance of each descriptor according to this analysis is: molecular volume, molecular weight and dipole moment, respectively. These descriptors appear good information related to different structure of sulphanilamide Schiff bases can participate in their inhibitor activity [17], anticarbonic anhydrase [18], the best corrosion inhibition behavior against the corrosion of mild steel in acid [4] and electrical conductivity [19]. Literature survey reveals that no work has been reported on thermal decomposition of sulfonamide Schiff's base under non-isothermal decomposition in the presence of dynamic oxygen atmosphere. This prompted us to carry out the synthesis, spectral characterization and thermal studies of 4-((Naphthalen-1-ylmethylene) amino)-benzene Sulfonamide (NMABS).

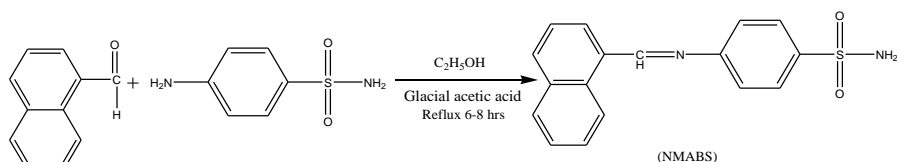
MATERIALS AND METHODS

In the present work, 4-aminobenzenesulfonamide and α -naphthaldehyde were purchased from Aldrich chemicals; glacial acetic acid and other reagents procured from S.D. Fine Chemicals and were used as received. Analytical Thin Layer Chromatography (TLC) was performed on pre-coated plastic sheets of silica gel G/UV-254 of 0.2 mm thickness. Melting points of the synthesized compound was determined in open-glass capillaries on a Mettler FP51 melting point apparatus and recorded in °C without correction. Elemental analyses were performed in Eurovector EuroEA3000 at Central Leather Research Institute (CLRI), Chennai, India. Fourier Transform Infrared (FT-IR) measurement was done as KBr pellet for solids using Shimadzu-2010 FT-IR spectrophotometer. The Proton Nuclear Magnetic Resonance (¹H-NMR) and Carbon-Carbon-13 Nuclear Magnetic Resonance (¹³C-NMR) spectra were recorded in Deuterated Dimethyl Sulfoxide (DMSO-d₆) using Tetramethylsilane (TMS) as internal standard with Bruker 400 MHz and 100 MHz high resolution NMR spectrometer.

The simultaneous Thermo Gravimetric (TG) and Difference Thermo Gravimetry (DTG) curves were obtained with the thermal analysis system model Perkin Elmer TGA 4000 V1.04. TGA/DTG at National Institute of Technology, Tiruchirappalli, India. The TG analysis of NMABS was carried out under dynamic oxygen atmosphere (100 ml/min⁻¹) in a 180 µl ceramic pan with a sample at the heating rates of 10, 15 and 20 K/min⁻¹ from 35-700°C. The sample temperature controlled by thermocouple, did not exhibit any systematic deviation from the preset linear temperature program. The kinetic parameters E_a and A were calculated using Microsoft Excel Software[®].

Synthesis of 4-((naphthalen-1-ylmethylene)amino)benzene sulfonamide

The Schiff's base was obtained by refluxing equimolar quantities of α-naphthaldehyde (1.35 ml, 0.01 mol), 4-aminobenzenesulfonamide (1.72 g, 0.01 mol) and few drops of glacial acetic acid in 25 ml of ethanol and heated on a water bath for 6-8 h. After the completion of the reaction, as monitored by TLC, the resulting solution was cooled to room temperature, and then poured into crushed ice with constant stirring. The precipitate was filtered and washed with cold water. The solid product was collected through filtration and then dried using drying oven at 80°C, recrystallized using ethanol to obtain the yield of product (Scheme 1) 89%.



Scheme 1: 4-((naphthalen-1-ylmethylene)amino)benzene sulfonamide

4-((Naphthalen-1-ylmethylene)-amino)-benzene sulfonamide

Yellow powdery solid; mp 110°C; Calculated (%) for C₁₇H₁₄N₂O₂S: C, 65.79; H, 4.55; N, 9.03 Found (%): C, 65.81; H, 4.56; N, 9.01. FT-IR (KBr) (cm⁻¹): 3309 (NH₂), 2989 (CH), 1581 (C=N), 1506 (C=C), 1153 (O=S=O), 840 (C-S) (Figure 1); ¹H-NMR (DMSO-*d*₆), δ ppm: 9.20 (s 1H, CH), 7.50-8.19 (m, 1H, Ar-H + SO₂NH₂) (Figure 2); ¹³C-NMR (DMSO-*d*₆), δ ppm: 122.28, 124.99, 125.34, 126.18, 126.30, 127.30, 127.76, 127.90, 128.59, 129.55, 129.62, 129.86, 131.47, 131.72, 131.88, 133.39, 134.36, 136.08 (aromatic carbons), 142.12 (C-S=O), 155.62 (C-N), 163.40 (C=N) (Figure 3).

Theoretical background

Model free methods

Friedman method [20] is a differential method and is one of the first isoconversional method. The model according to logarithmic form is given as Eqns. 1 and 2:

$$\beta \left[\frac{d\alpha}{dt} \right] = A \exp \left(-\frac{E}{RT} \right) f(\alpha) \quad (1)$$

$$\ln \left[\beta \frac{d\alpha}{dT} \right] = \ln [A_\alpha f(\alpha)] - \frac{E_a \alpha}{RT_\alpha} \quad (2)$$

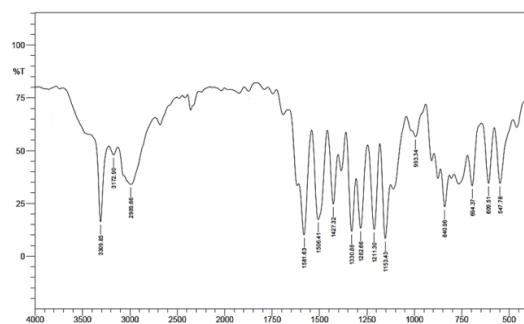


Figure 1: FT-IR spectrum of NMABS in KBr disc (cm⁻¹)

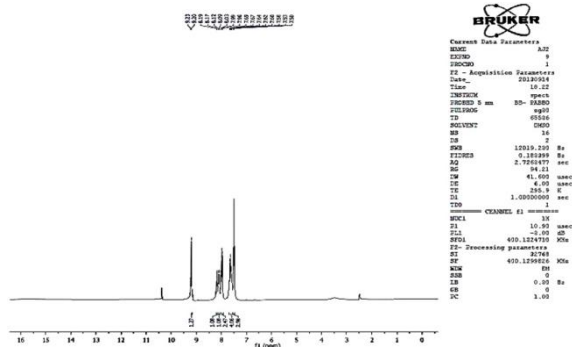


Figure 2: ¹H-NMR spectrum of NMABS in DMSO-*d*₆

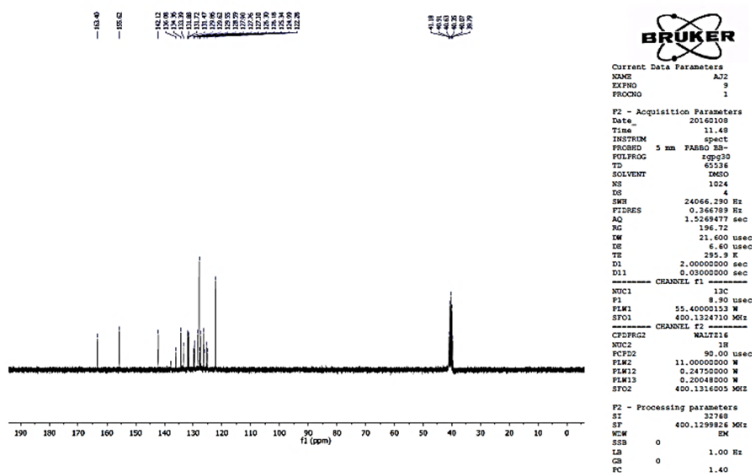


Figure 3: ^{13}C -NMR spectrum of NMABS in $\text{DMSO } d_6$

A plot of $\ln [\beta d\alpha/dT]$ (or $\ln \Delta\alpha/\Delta t$) versus $1/T$ (Eqn. 2) at each degree of conversion α value, activation energy (E_a) obtained from the slope of the plots. The isoconversional integral method suggested independently by Flynn and Wall [21] and Ozawa [22] uses Doyle's [23-25] approximation of $p(x)$. This method is based on the Eqn. 3:

$$\log \beta = \log \frac{AE_a}{Rg(\alpha)} - 2.315 - 0.4567 \frac{E_a}{RT} \quad (3)$$

For constant degree of conversion α , the left side of above equation against $1000/T$, obtained from thermograms recorded at several heating rates, should be a straight lines whose slope can be used to evaluate the apparent activation energy and Kissinger-Akahira-Sunose (KAS) [26,27] Eqn. 4:

$$\ln \left[\frac{\beta}{T^2} \right] = \ln \left[\frac{AR}{E_a g(\alpha)} \right] - \frac{E_a}{RT} \quad (4)$$

Thus, for $\alpha = \text{constant}$, the plot of $\ln (\beta/T^2)$ versus $(1/T)$ should be a straight line whose slope can be used to evaluate the apparent activation energy.

Model fitting method

There are several non-isothermal model-fitting methods are available and the most popular one is the Coats-Redfern method [28] which has been successfully used for studying the kinetics of dehydration and decomposition of different solid substances [28,29]. The kinetic parameters can be obtained from modified Coats-Redfern Eqn. 5:

$$\ln \left[\frac{g(\alpha)}{T^2} \right] = \ln \left[\frac{AR}{\beta E_a} \left(1 - \left(\frac{2RT_{\text{exp}}}{E_a} \right) \right) \right] - \frac{E_a}{RT} \approx \ln \left[\frac{AR}{\beta E_a} \right] - \left(\frac{E_a}{RT} \right) \quad (5)$$

Where, $g(\alpha)$ is an integral form of the conversion function, the expression of which depends on the kinetic model occurring of the reaction. If the correct $g(\alpha)$ function is used, a plot of $\ln [g(\alpha)/T^2]$ against $1/T$ gives a straight line, in further particular reaction model whose slope and intercept allow us to calculate E_a and the pre-exponential factor A.

Invariant kinetic parameters (IKP) method

Criado and Morales [30] observed that almost any $\alpha = \alpha(T)$ or $(d\alpha/dt) = (d\alpha/dt)(T)$ experimental curve may be correctly described by several conversion functions. Further, the values of the activation energy obtained for various $f(\alpha)$ for single non-isothermal curve are correlated through the compensation effect.

$$\ln A_{\text{inv}} = a_\beta + b_\beta E_{\text{inv}} \quad (6)$$

The above Eqn. 6 represents a linear relationship between $\ln A_{\text{inv}}$ and E_{inv} [31] any increase in the magnitude of one parameter is offset, or compensated, by appropriate increase of the other. Plotting $\ln A_{\text{inv}}$ versus E_{inv} for different heating rates, the compensation effect parameters a_β and b_β were obtained. These parameters follow an Eqn. 7:

$$a_\beta = \ln A_{\text{inv}} - b_\beta E_{\text{inv}} \quad (7)$$

The plot of a_β versus b_β gives the true values [32] of E_{inv} and $\ln A_{\text{inv}}$ obtained from the slope and intercept of the plot, respectively.

Determination of pre-exponential (frequency) factor and decomposition kinetic model

Based on the apparent activation energy (E_a) and reaction (conversion) model [$g(\alpha)$], the value of A can be calculated from Eqn. 8, in accordance with dependence $g(\alpha)$ versus $E_a p(x)/R\beta$.

$$g(\alpha) = \frac{AE_a}{R\beta} p(x) \quad (8)$$

Where, $g(\alpha)$ is the integral form of the reaction model and $p(x)$ is the temperature integral, for $x=E_a/RT$, which does not have analytical solution. For calculating the value of A for the investigated decomposition process, the fourth rational expression of Senum and Yang [33] for $p(x)$ function was used. From the plot of $g(\alpha)$ versus $E_a p(x)/R\beta$, frequency factor (A) can be determined from the slope of the plot.

Thermodynamic parameters

The kinetic parameters, energy of activation (E_a) and pre-exponential factor (A) are obtained from Kissinger single point [26,34,35] kinetic method which uses the Eqn. 9:

$$\ln \left[\frac{\beta}{T_m^2} \right] = \ln \left[\frac{AR}{E_a} \right] - \frac{E_a}{RT_m} \quad (9)$$

Where, T_m is temperature that corresponds to the maximum of $d\alpha/dT$. This 'model-free' kinetic method can be applied with a reasonable approximation without being limited to n -order kinetics [36], providing a single E_a value for each decomposition step. For this reason, it is often defined as a Kissinger single point method. The reaction proceeds under conditions where thermal equilibrium is always maintained, then a plot of $\ln(\beta/T_m^2)$ versus $1/T_m$ gives a straight line with a slope equal to $-E_a/R$. The thermodynamic parameters were determined according to literature [36-38].

RESULTS AND DISCUSSION

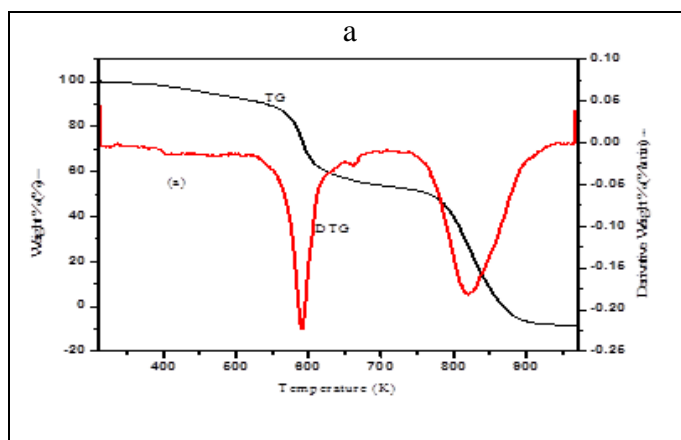
Non-isothermal TG and DTG

The thermograms of pure NMABS recorded in a dynamic oxygen atmosphere at different heating rates of 10, 15 and 20 K/min⁻¹ are presented in Figure 4. The TG curves at different heating rates showed that the decomposition of the NMABS proceeds in a two steps. DTG curves show that decomposition process is endothermic nature. The weight loss was observed in TG curves on heating of NMABS from 473 to 973 K. All the thermogravimetric curves are asymmetric and the maximum moves to higher temperatures with increase in heating rate. The decomposition process for NMABS, first stage starts at 523 K and ends at 630 K with the mass loss of ~41% (cal. 46.6%) and second stage starts at 630 K and ends at 925 K with the mass loss of ~59% (cal. 53.3%) which indicate removal of naphthyl and sulfonamide groups, respectively.

Model-free analysis

All results of non-isothermal TG analyses under an oxygen atmosphere and typical results of those under oxygen atmospheres are shown in Figure 4. The obtained TG analysis data for the described stages of the compound NMABS were analyzed to determine the activation energy for a different level of conversion using Eqn. 4. Slopes of the regression lines in the conversional plots for the each stage, which are shown in Figures 5 and 6, were used to calculate the activation energy at each degree of conversion.

Budrugaec [39] analyzed the procedural errors in the kinetic triplet [E_a , A, $f(\alpha)$] evaluation and proposed a general algorithm to be applied. The kinetic analysis must begin with the evaluation of the activation energy dependence on the conversion degree. When E_a does not depend on α , only a single reaction is involved, a unique kinetic triplet being expected to describe it. If E_a changes with α , then the process is complex. Vyazovkin and Lesnikovich [40], Vyazovkin [41] established an algorithm to identify the type of complex process. When, E_a increases with conversion degree, the process involves parallel reactions.



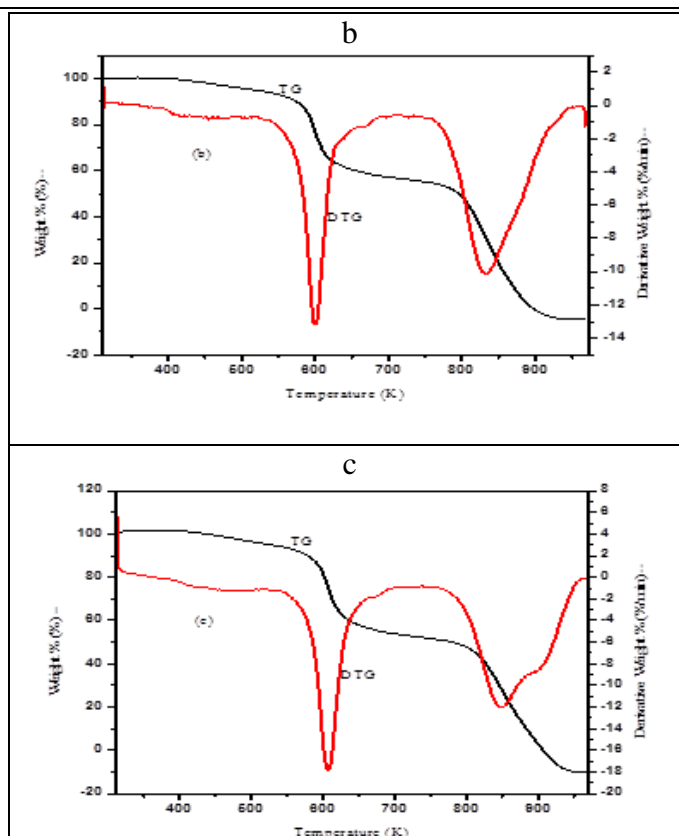


Figure 4: TG and DTG Curves of NMABS at (a) 10 K/min⁻¹, (b) 15 K/min⁻¹ and (c) 20 K/min⁻¹ heating rates in oxygen atmosphere

When, E_a decreases and the shape of its evolution is concave, then the process has reversible stages. For decreasing convex shape, the process changes the limiting stage. Since, from isoconversional methods the pre-exponential factor and conversion function cannot be determined at the same time, advanced methods have been developed. If the isoconversional activation energy remains constant, no variation of the pre-exponential factor should be encountered.

Flynn-Wall-Ozawa, Kissinger-Akahira-Sunose and Friedman isoconversional methods (Tables 1 and 2) were used to determine apparent activation energy E_a . E_a values constant slightly in the conversion range of $0.05 \leq \alpha \leq 0.95$. The applied isoconversional methods do not suggest a direct way for evaluating either the pre-exponential factor (A) or the analytical form of the reaction model $f(\alpha)$, for the investigated decomposition process of NMABS. Furthermore, the results indicate the independence of the apparent activation energy (E_a) on the extent of conversion (α). It helps not only to disclose the complexity of a decomposition process, but also to identify its kinetic scheme.

The results are presented in Tables 1 and 2 (Figures 7 and 8) for the first and second stages decomposition of NMABS, the values of the apparent activation energies obtained by KAS method ($E_a=86.08 \pm 2.33$ kJ/mol⁻¹) is lower than (FWO, $E_a=91.47 \pm 2.64$ kJ/mol⁻¹; Friedman, 90.97 ± 0.19 kJ/mol⁻¹) and for Stage II, the average value of FWO method are almost equal to KAS method ($E_a=261.92 \pm 5.44$ kJ/mol⁻¹, FWO; $E_a=261.34 \pm 5.37$ kJ/mol⁻¹, KAS) and higher value by Friedman method ($E_a=267.04 \pm 0.34$ kJ/mol⁻¹). It is important to note that the shape of the curves, E_a versus α corresponding to the isoconversional methods is almost the same (Figures 7 and 8). As seen from the E_a versus α curve, the E_a values remain constant with an increase α values.

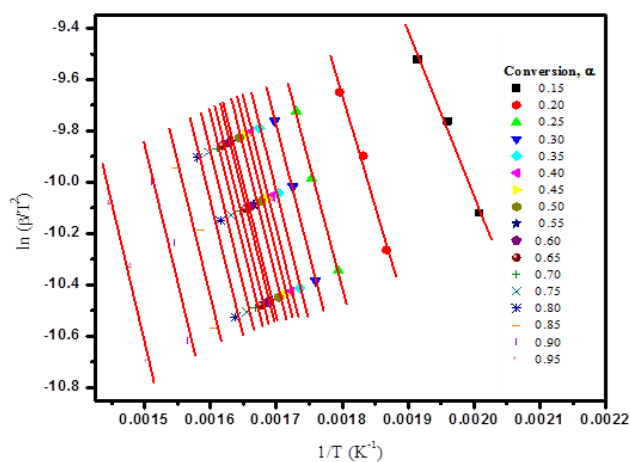


Figure 5: Slopes of the regression lines in the isoconversional plots for NMABS (Stage I)

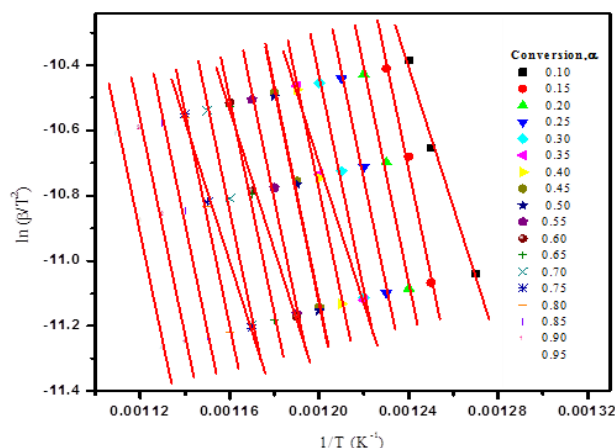


Figure 6: Slopes of the regression lines in the isoconversional plots for NMABS (Stage II)

Table 1: Temperatures corresponding to the same degree of conversion at different heating rates for NMABS (Stage I)

α	Temperature (K)			FWO method			KAS method			Friedman method	
	(K/min ⁻¹)	(K/min ⁻¹)	(K/min ⁻¹)	E _a (kJ/mol ⁻¹)	ln A (A/min ⁻¹)	-r	E _a (kJ/mol ⁻¹)	ln A (A/min ⁻¹)	-r	E _a (kJ/mol ⁻¹)	-r
0.25	557.43	570.27	577.94	85.32	14.66	0.998	80.3	16.13	0.998	-	-
0.3	568.36	579.7	589.17	88.36	14.95	0.999	83.32	16.45	0.999	90.87	0.955
0.35	576.17	587.11	597.21	89.8	14.99	0.998	84.7	16.49	0.997	90.86	0.983
0.4	580.86	590.85	602.01	90.35	14.95	0.993	85.2	16.45	0.991	91.03	0.88
0.45	583.98	593.33	605.18	90.52	14.89	0.988	85.32	16.38	0.985	90.81	0.865
0.5	587.11	596.48	608.41	91.03	14.89	0.988	85.81	16.39	0.985	91.29	0.984
0.55	591.79	600.38	613.15	91.17	14.78	0.98	85.87	16.26	0.975	90.97	0.877
0.6	593.36	601.95	614.77	91.41	14.77	0.98	86.09	16.25	0.975	91.48	0.973
0.65	596.48	605.07	618.01	91.78	14.75	0.979	86.43	16.23	0.974	90.9	0.971
0.7	599.6	608.2	621.26	92.13	14.72	0.979	86.74	16.19	0.974	90.82	0.971
0.75	604.29	612.88	626.15	92.58	14.66	0.978	87.14	16.13	0.972	91.01	0.967
0.8	610.54	619.13	632.7	93.05	14.55	0.977	87.53	16.01	0.971	90.7	0.965
0.85	623.04	630.85	645.63	93.29	14.23	0.965	87.57	15.65	0.957	90.97	0.918
0.9	638.66	647.25	662.26	94.72	14.03	0.97	88.81	15.43	0.963	90.92	0.975
0.95	665.21	676.15	690.92	96.68	13.61	0.985	90.41	14.96	0.981	90.98	0.995
Mean				91.47 ± 2.64			86.08 ± 2.33			90.97 ± 0.19	

From the E_a value, we concluded that rate of decomposition in Stage II is slower when compare to Stage I.

Model-fitting analysis

After model-free analysis is performed, model-fitting can be done in these conversion regions where apparent activation energy is approximately constant which indicate that a single mechanism may fit. The non-isothermal kinetic data of NMABS at 0.20 ≤ α ≤ 0.95 where model-free analysis indicates that activation energy approximately constant, were then fitted into each of the 15 models [28] listed in Tables 3 and 4. Arrhenius parameters (E_a, ln A) for decomposition process, exhibit strong dependence on the reaction model chosen. The values of E_a (mean values are calculated by Friedman method) for NMABS coincide with the values calculated by Coats-Redfern method. Based on the kinetic data, it is concluded that the decomposition occurred in a single mechanism which is also confirmed by invariant kinetic parameters method.

Invariant kinetic parameters (IKP) method

Criado and Morales [30] have reported that almost any α=α(T) or (da/dt) (T) experimental curve may be correctly described by several conversion functions. The use of an integral or differential model-fitting method leads to different values of the activation parameters. Although obtained with high accuracy, the values change with different heating rates and conversion functions. In the present study, the Coats-Redfern model-fitting method was chosen [28]. The apparent activation parameters obtained for each heating rate of the best-fitting kinetic models are presented in Tables 3 and 4.

Table 2: Temperatures corresponding to the same degree of conversion at different heating rates for NMABS (Stage II)

α	Temperature (K)			FWO method			KAS method			Friedman method	
	(K/min ⁻¹)	(K/min ⁻¹)	(K/min ⁻¹)	E _a (kJ/mol ⁻¹)	ln A (A/min ⁻¹)	-r	E _a (kJ/mol ⁻¹)	ln A (A/min ⁻¹)	-r	E _a (kJ/mol ⁻¹)	-r
0.2	807.4	814.82	821.98	249.72	33.32	0.997	249.11	36.27	0.996	-	-
0.25	812.87	820.68	827.43	253.71	33.65	0.999	253.21	36.62	0.999	266.78	0.998
0.3	818.34	825.76	832.94	256.11	33.76	0.997	255.65	36.73	0.996	267.06	0.978
0.35	822.24	830.05	836.87	258.32	33.89	0.999	257.9	36.88	0.998	266.88	0.995
0.4	826.93	834.74	841.64	259.84	33.89	0.998	259.42	36.88	0.998	266.81	0.997
0.45	830.83	838.64	845.62	260.86	33.86	0.998	260.44	36.84	0.998	266.54	0.997
0.5	835.52	843.33	850.41	262.02	33.81	0.998	261.57	36.79	0.998	267.39	0.996
0.55	839.43	847.24	854.41	262.86	33.75	0.998	262.39	36.73	0.997	267.58	0.996
0.6	843.33	851.53	858.39	263.99	33.73	0.999	263.51	36.7	0.999	267.36	0.995
0.65	848.02	856.22	863.21	264.68	33.61	0.999	264.16	36.58	0.999	267.78	0.997
0.7	853.49	861.3	868.85	264.85	33.39	0.997	264.25	36.35	0.996	266.9	0.972
0.75	858.17	865.98	873.67	265.26	33.23	0.996	264.6	36.18	0.996	267.21	0.993
0.8	863.64	871.84	879.31	266.09	33.1	0.998	265.38	36.05	0.998	266.75	1
0.85	869.89	877.7	885.76	265.91	32.8	0.995	265.09	35.73	0.994	266.82	0.971
0.9	876.14	881.06	891.39	264.45	32.38	0.957	263.45	35.28	0.952	267.06	0.594
0.95	883.95	890.59	899.71	272.16	33.08	0.983	271.42	36.02	0.981	266.82	0.994
Mean				261.92 ± 5.44			261.34 ± 5.37			267.04 ± 0.34	

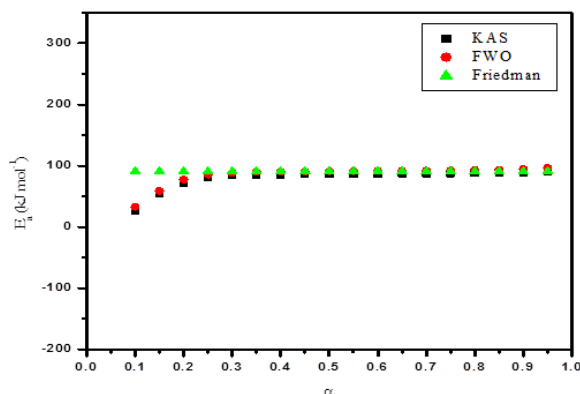


Figure 7: E_a versus α plot for the decomposition of NMABS (Stage I) under non-isothermal condition in oxygen atmosphere

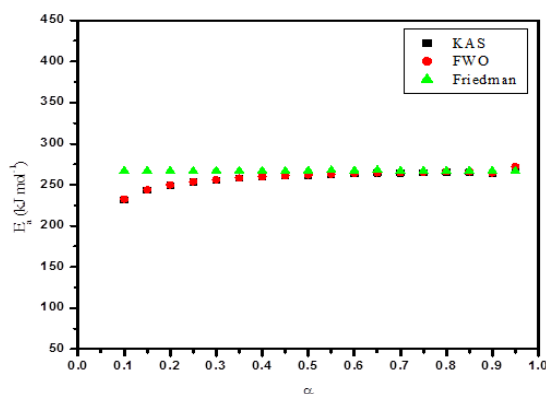


Figure 8: E_a versus α plot for the decomposition of NMABS (Stage II) under non-isothermal condition in oxygen atmosphere

The apparent kinetic parameters for the thermal decomposition in airflow for NMABS are represented in ln A versus E_a (Figures 9 and 10). The evaluation of the invariant kinetic parameters is performed using the super correlation in Eqn. 7 (Table 5).

Table 3: Apparent activation parameters by Coats-Redfern method for each heating rate for NMABS (Stage I)

Kinetic model g(α)	$\beta=10$ K/min ⁻¹			$\beta=15$ K/min ⁻¹			$\beta=20$ K/min ⁻¹		
	E _a (kJ/mol ⁻¹)	ln A (A/min ⁻¹)	-r	E _a (kJ/mol ⁻¹)	ln A (A/min ⁻¹)	-r	E _a (kJ/mol ⁻¹)	ln A (A/min ⁻¹)	-r
$\alpha^{(1/3)}$ (P2)	5.92	-3.02	0.855	8.74	-1.71	0.907	10.52	-0.97	0.919
$\alpha^{(1/2)}$ (P3)	1.07	-5.61	0.421	2.80	-3.93	0.722	3.86	-3.17	0.786
$-\ln(1-\alpha)$ (F1)	29.13	3.45	0.902	37.64	5.69	0.932	43.62	7.11	0.953
$(1-\alpha)^{-1}-1$ (F2)	41.53	6.97	0.846	53.67	9.90	0.885	62.66	11.86	0.917
$0.5[(1-\alpha)^{-2}-1]$ (F3)	56.87	11.17	0.797	73.57	14.97	0.840	86.34	17.60	0.877
α^2 (D1)	58.23	16.57	0.964	71.49	19.63	0.972	80.36	21.48	0.975
$[(1-\alpha)\ln(1-\alpha)+\alpha]$ (D2)	54.19	7.62	0.947	68.05	10.81	0.961	77.43	12.76	0.969
$[1-(1-\alpha)^{1/3}]^2$ (D3)	60.20	7.76	0.934	75.78	11.28	0.953	86.59	13.48	0.966
$(1-2\alpha/3)-(1-\alpha)^{2/3}$ (D4)	59.56	7.31	0.936	74.96	10.81	0.954	86.16	13.09	0.973
$[-\ln(1-\alpha)]^{1/2}$ (A2)	10.27	-1.34	0.837	14.31	0.14	0.895	17.10	1.06	0.929
$[-\ln(1-\alpha)]^{1/3}$ (A3)	3.91	-3.57	0.677	6.44	-2.21	0.816	8.15	-1.42	0.880
$[-\ln(1-\alpha)]^{1/4}$ (A4)	0.84	-5.73	0.258	2.64	-3.85	0.615	3.84	-3.00	0.761
$[1-(1-\alpha)^{1/2}]$ (R2)	24.34	1.34	0.924	31.48	3.32	0.947	36.34	4.54	0.960
$[1-(1-\alpha)^{1/3}]$ (R3)	23.00	1.22	0.930	29.77	3.13	0.950	34.31	4.29	0.961

The invariant kinetic parameters are $E_{inv}=62.11 \pm 0.48$ kJ/mol⁻¹ and $\ln A_{inv}=10.03 \pm 0.11$ (A/min⁻¹) are obtained from linear plot with $r=0.999$. For these groups, the invariant activation energy is slightly above 62.11 ± 0.48 kJ/mol⁻¹ close to 86.08 ± 2.33 kJ/mol⁻¹ obtained by KAS method. Thus, for second stage decomposition (Table 6 and Figure 10) AKM-{D1}, the invariant kinetic parameters $E_{inv}=266.35 \pm 23.57$ kJ/mol⁻¹ and $\ln A_{inv}=36.05 \pm 3.40$ (A/min⁻¹) were obtained from linear plot with $r=0.996$ (Table 7 and Figure 11). For these groups, the invariant activation energy is slightly lower 261.34 ± 5.37 and 261.92 ± 5.44 kJ/mol⁻¹ (KAS and FWO methods), close to value obtained by Friedman method $E_a=267.04 \pm 0.34$ kJ/mol⁻¹. From the apparent activation energy values, we confirmed that the rate of decomposition of first stage is faster when comparing to second stage of NMABS.

Table 4: Apparent activation parameters by Coats-Redfern method for each heating rate for NMABS (Stage II)

Kinetic model g(α)	$\beta=10$ K/min ⁻¹			$\beta=15$ K/min ⁻¹			$\beta=20$ K/min ⁻¹		
	E _a (kJ/mol ⁻¹)	ln A (A/min ⁻¹)	-r	E _a (kJ/mol ⁻¹)	ln A (A/min ⁻¹)	-r	E _a (kJ/mol ⁻¹)	ln A (A/min ⁻¹)	-r
$\alpha^{(1/3)}$ (P2)	59.28	5.82	0.968	61.19	6.44	0.971	61.34	6.65	0.964
$\alpha^{(1/2)}$ (P3)	34.89	1.92	0.958	36.13	2.48	0.963	36.17	2.71	0.954
$\alpha^{(3/2)}$ (P4)	22.77	-0.18	0.945	23.67	0.35	0.951	23.67	0.59	0.940
$-\ln(1-\alpha)$ (F1)	186.23	25.24	0.998	191.37	26.15	0.998	192.79	26.38	0.997
$(1-\alpha)^{-1}-1$ (F2)	264.97	37.49	0.988	271.69	38.51	0.987	274.78	38.89	0.990
$0.5[(1-\alpha)^{-2}-1]$ (F3)	363.43	52.64	0.964	372.07	53.81	0.961	377.33	54.37	0.967
α^2 (D1)	297.09	48.60	0.979	305.41	49.83	0.981	306.56	49.89	0.976
$[(1-\alpha)\ln(1-\alpha)+\alpha]$ (D2)	307.12	41.41	0.986	315.82	42.67	0.987	317.29	42.75	0.984
$[1-(1-\alpha)^{1/3}]^2$ (D3)	344.79	45.72	0.994	354.32	47.05	0.995	356.51	47.19	0.993
$(1-2\alpha/3)-(1-\alpha)^{2/3}$ (D4)	337.64	44.37	0.984	347.27	45.72	0.986	349.16	45.83	0.983
$[-\ln(1-\alpha)]^{1/2}$ (A2)	86.24	10.29	0.997	88.75	10.95	0.998	89.39	11.21	0.997
$[-\ln(1-\alpha)]^{1/3}$ (A3)	52.46	5.00	0.997	54.08	5.59	0.998	54.45	5.85	0.996
$[-\ln(1-\alpha)]^{1/4}$ (A4)	36.25	2.34	0.996	37.45	2.88	0.997	37.70	3.14	0.996
$[1-(1-\alpha)^{1/2}]$ (R2)	156.27	19.83	0.990	160.77	20.68	0.991	161.61	20.87	0.988
$[1-(1-\alpha)^{1/3}]$ (R3)	147.99	18.79	0.985	152.30	19.63	0.987	153.00	19.81	0.984

Table 5: Compensation effect parameters for several combinations of kinetic models for NMABS (Stage I)

β (K/min ⁻¹)	AKM			AKM-{D1}		
	a_β (A/min ⁻¹)	b_β (mol/J ⁻¹)	r	a_β (A/min ⁻¹)	b_β (mol/J ⁻¹)	r
10	-4.9122	0.2631	0.939	-4.5975	0.2355	0.971
15	-3.9289	0.2412	0.953	-3.6247	0.2197	0.981
20	-3.4335	0.2303	0.959	-3.1543	0.2123	0.985
β (K/min ⁻¹)	AKM-{D1, D2}			AKM-{D1, D2, D3}		
	a_β (A/min ⁻¹)	b_β (mol/J ⁻¹)	r	a_β (A/min ⁻¹)	b_β (mol/J ⁻¹)	r
10	-4.6200	0.2380	0.968	-4.8033	0.2535	0.973
15	-3.6472	0.2217	0.980	-3.8321	0.2333	0.983
20	-3.1761	0.2139	0.984	-3.3573	0.2238	0.986
β (K/min ⁻¹)	AKM-{D1, D2, D3, D4}			AKM-{D1, D2, D3, D4, P3}		
	a_β (A/min ⁻¹)	b_β (mol/J ⁻¹)	r	a_β (A/min ⁻¹)	b_β (mol/J ⁻¹)	r
10	-5.2347	0.2906	0.995	-5.0501	0.2856	0.995
15	-4.2590	0.2606	0.998	-4.1483	0.2583	0.998
20	-3.7753	0.2466	0.998	-3.6805	0.2449	0.998
β (K/min ⁻¹)	AKM-{D1, D2, D3, D4, P3, A4}			AKM-{D1, D2, D3, D4, P3, A4, R2}		
	a_β (A/min ⁻¹)	b_β (mol/J ⁻¹)	r	a_β (A/min ⁻¹)	b_β (mol/J ⁻¹)	r
10	-4.7104	0.2764	0.997	-4.6139	0.2764	0.999
15	-4.0060	0.2553	0.998	-3.9014	0.2552	0.999
20	-3.5842	0.2432	0.998	-3.4759	0.2430	0.999
β (K/min ⁻¹)	AKM-{D1, D2, D3, D4, P3, A4, R2, R3}			AKM-{D1, D2, D3, D4, P3, A4, R2, R3, A2}		
	a_β (A/min ⁻¹)	b_β (mol/J ⁻¹)	r	a_β (A/min ⁻¹)	b_β (mol/J ⁻¹)	r
10	-4.5173	0.2760	1.000	-4.6623	0.2788	1.000
15	-3.7934	0.2548	1.000	-3.9169	0.2566	1.000
20	-3.3633	0.2426	1.000	-3.4799	0.2441	1.000

Table 6: Compensation effect parameters for several combinations of kinetic models for NMABS (Stage II)

β (K/min ⁻¹)	AKM			AKM-{D1}		
	a_β (A/min ⁻¹)	b_β (mol/J ⁻¹)	r	a_β (A/min ⁻¹)	b_β (mol/J ⁻¹)	r
10	-3.0311	0.1500	0.993	-2.8308	0.1459	0.998
15	-2.6103	0.1485	0.993	-2.4062	0.1445	0.998
20	-2.3370	0.1472	0.993	-2.1410	0.1433	0.998
β (K/min ⁻¹)	AKM-{D1, D2}			AKM-{D1, D2, D4}		
	a_β (A/min ⁻¹)	b_β (mol/J ⁻¹)	r	a_β (A/min ⁻¹)	b_β (mol/J ⁻¹)	r
10	-2.8559	0.1463	0.998	-3.0521	0.1489	0.998
15	-2.4316	0.1449	0.998	-2.6302	0.1475	0.998
20	-2.1660	0.1437	0.998	-2.3613	0.1462	0.998
β (K/min ⁻¹)	AKM-{D1, D2, D4, F1}			AKM-{D1, D2, D4, F1, F2}		
	a_β (A/min ⁻¹)	b_β (mol/J ⁻¹)	r	a_β (A/min ⁻¹)	b_β (mol/J ⁻¹)	r
10	-3.0807	0.1488	0.998	-3.0559	0.1477	0.999
15	-2.6586	0.1473	0.998	-2.6335	0.1463	0.999

20	-2.3899	0.1461	0.999	-2.3649	0.1450	0.999
β (K/min ⁻¹)	AKM-{D1, D2, D4, F1, F2, F3}			AKM-{D1, D2, D4, F1, F2, F3, A2}		
	a_β (A/min ⁻¹)	b_β (mol/J ⁻¹)	r	a_β (A/min ⁻¹)	b_β (mol/J ⁻¹)	r
10	-2.6321	0.1416	0.999	-2.7399	0.1417	1.000
15	-2.2102	0.1403	0.999	-2.3177	0.1405	1.000
20	-1.9373	0.1391	0.999	-2.0451	0.1392	1.000
β (K/min ⁻¹)	AKM-{D1, D2, D4, F1, F2, F3, A2, R2}			AKM-{D1, D2, D4, F1, F2, F3, A2, R2, R3}		
	a_β (A/min ⁻¹)	b_β (mol/J ⁻¹)	r	a_β (A/min ⁻¹)	b_β (mol/J ⁻¹)	r
10	-2.7700	0.1414	1.000	-2.8327	0.1410	1.000
15	-2.3476	0.1402	1.000	-2.4099	0.1397	1.000
20	-2.0750	0.1389	1.000	-2.1375	0.1385	1.000
β (K/min ⁻¹)	AKM-{D1, D2, D4, F1, F2, F3, A2, R2, R3, P4}					
	a_β (A/min ⁻¹)	b_β (mol/J ⁻¹)	r			
10	-2.6544	0.1403	1.000			
15	-2.2329	0.1391	1.000			
20	-1.9594	0.1379	1.000			

Table 7: IKP for several combinations of kinetic models for NMABS (Stages I and II)

Compounds	Kinetic model	E_{inv} (kJ/mol ⁻¹)	$\ln A_{inv}$ (A/min ⁻¹)	r
NMABS (Stage I)	AKM	45.06	6.94	1.000
	AKM-{D1}	62.11	10.03	0.999
	AKM-{D1, D2}	59.88	9.63	1.000
	AKM-{D1, D2, D3}	48.59	7.51	0.999
	AKM-{D1, D2, D3, D4}	33.07	4.37	0.999
	AKM-{D1, D2, D3, D4, P3}	33.56	4.53	0.999
	AKM-{D1, D2, D3, D4, P3, A4}	33.86	4.65	0.999
	AKM-{D1, D2, D3, D4, P3, A4, R2}	34.02	4.79	0.999
	AKM-{D1, D2, D3, D4, P3, A4, R2, R3}	34.51	5.00	0.999
	AKM-{D1, D2, D3, D4, P3, A4, R2, R3, A2}	34.02	4.82	0.999
	AKM	248.72	34.29	0.997
	AKM-{D1}	266.35	36.05	0.996
	AKM-{D1, D2}	266.39	36.13	0.996
	AKM-{D1, D2, D4}	256.43	35.15	0.994
NMABS (Stage II)	AKM-{D1, D2, D4, F1}	256.90	35.16	0.998
	AKM-{D1, D2, D4, F1, F2}	256.51	34.85	0.994
	AKM-{D1, D2, D4, F1, F2, F3}	278.57	36.83	0.995
	AKM-{D1, D2, D4, F1, F2, F3, A2}	276.97	36.54	0.989
	AKM-{D1, D2, D4, F1, F2, F3, A2, R2}	277.05	36.44	0.989
	AKM-{D1, D2, D4, F1, F2, F3, A2, R2, R3}	278.73	36.49	0.995
	AKM-{D1, D2, D4, F1, F2, F3, A2, R2, R3, P4}	289.58	38.00	0.993

The plot of a_β versus b_β , obtained for three different rates, is a straight line, from which $\ln A_{inv}$ and E_{inv} are determined. The detailed images of the plots for NMABS (stages I, II) (Figures 9 and 10), (undersized figure in up-left corner) show the incompatibility of few models among all other conversion functions, although it's apparent parameters were obtained with high correlation coefficients.

In NMABS (stage I) AKM-{D1}, the plot of $\ln A$ versus E_a has the highest correlation coefficient, from the slope (b_p) and intercept (a_p) values and we calculated $\ln A_{inv}$ and E_{inv} (Table 5 and Figure 9) ($r=0.999$) (Table 7 and Figure 11).

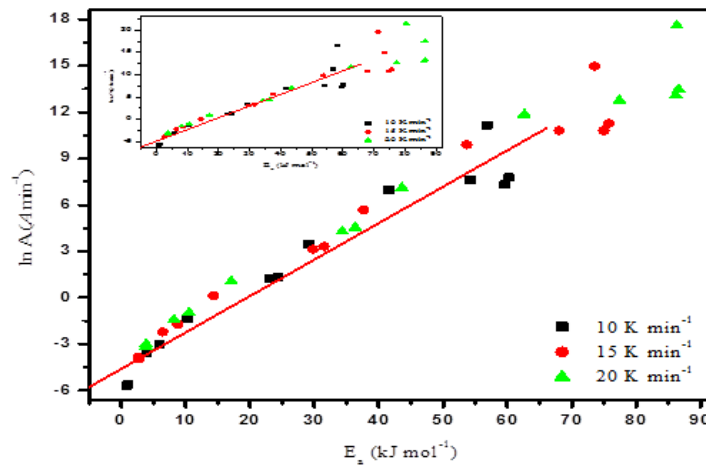


Figure 9: $\ln A$ versus E_a plot for AKM-{D1} combination at $\beta=10, 15$ and 20 K/min^{-1} for NMABS (Stage I)

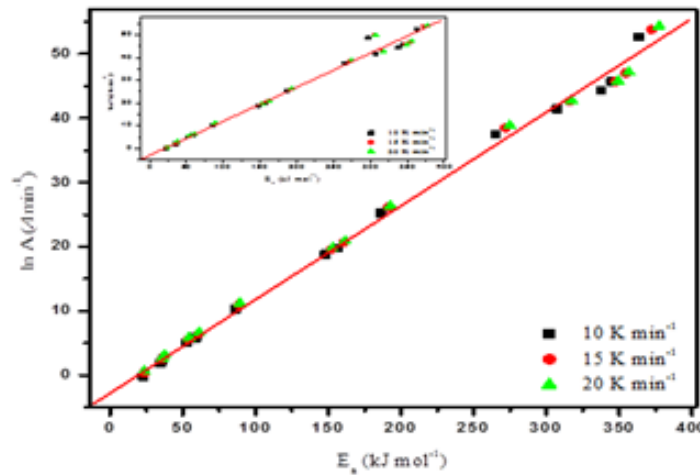


Figure 10: $\ln A$ versus E_a plot for AKM-{D1} combination at $\beta=10, 15$ and 20 K/min^{-1} for NMABS (Stage II)

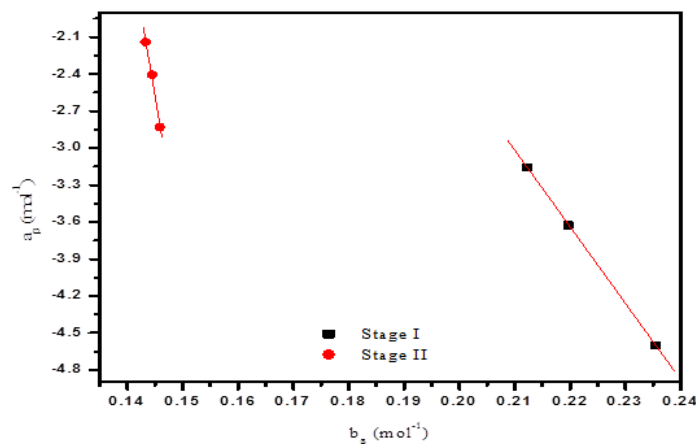


Figure 11: Super correlation (compensation effect parameters) plot for the best combination models ($\beta=10, 15$ and 20 K min^{-1})

Kinetic model determination

The most probable kinetic model for decomposition process of NMABS (Stages I and II) is F2 and D3 models. By introducing the derived reaction model $g(\alpha)=[(1-\alpha)^{-1}-1]$ and $g(\alpha)=[1-(1-\alpha)^{1/3}]^2$ the following equations [42] are obtained.

$$[(1-\alpha)^{-1}-1] = \frac{AE_a}{R\beta} p(x) \quad (10)$$

$$[1-(1-\alpha)^{1/3}]^2 = \frac{AE_a}{R\beta} p(x) \quad (11)$$

The plot of $[(1-\alpha)^{-1}-1]$ or $[1-(1-\alpha)^{1/3}]^2$ against $E_a p(x)/R\beta$ at different heating rates is constructed in Figures 12 and 13. For second order model (F2) $E_a=90.97 \pm 0.19 \text{ kJ/mol}^{-1}$ and the pre-exponential (frequency) factor was found to be $A=2.26 \times 10^4 \text{ min}^{-1}$ ($\ln A=10.03$). This value of $\ln A$ is in good agreement with the average value of Friedman isoconversional intercept $\ln [A f(\alpha)]=10.15$ for stage I.

For 3-D Diffusion-Jander equation model (D3) $E_a=267.04 \pm 0.34 \text{ kJ/mol}^{-1}$ and the pre-exponential (frequency) factor was found to be $4.53 \times 10^{15} \text{ min}^{-1}$ ($\ln A=36.05$). The $\ln A$ value is in good agreement with the average value of Friedman isoconversional intercept $\ln [A f(\alpha)]=36.93$ for stage II. According to Eqn. 8, the kinetic equation for describing the non-isothermal decomposition process of NMABS (stages I and II) are given by:

$$\beta \frac{d\alpha}{dT} = 2.26 \times 10^4 \times \exp\left(-\frac{90.97}{RT}\right) (1-\alpha)^2 \quad (12)$$

$$\beta \frac{d\alpha}{dT} = 4.53 \times 10^{15} \times \exp\left(-\frac{267.04}{RT}\right) 2(1-\alpha)^{2/3} [1-(1-\alpha)^{1/3}]^{-1} \quad (13)$$

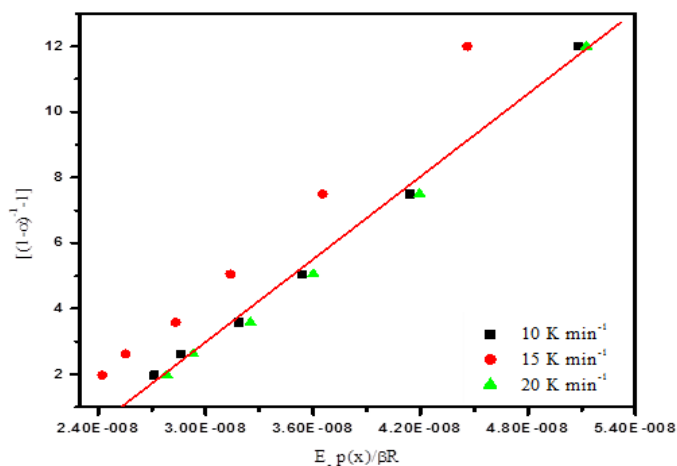


Figure 12: Determination of A value by plotting $[(1-\alpha)^{-1}-1]$ against $E_a p(x)/\beta R$ for the decomposition of NMABS at different heating rates (β) (Stage I)

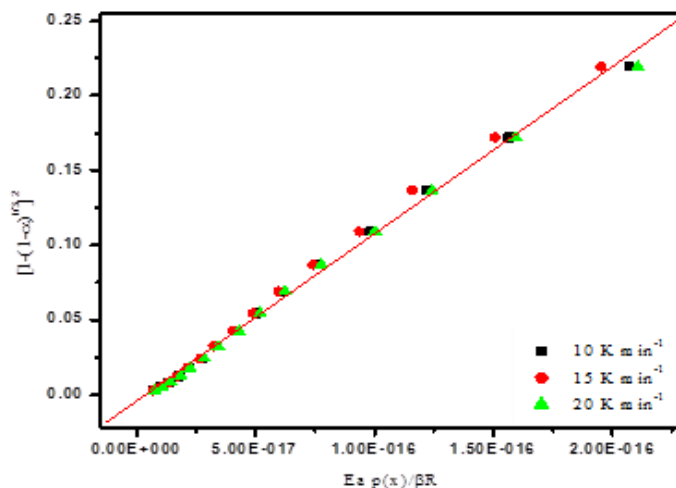


Figure 13: Determination of A value by plotting $[1-(1-\alpha)^{1/3}]^2$ against $E_a p(x)/\beta R$ for the decomposition of NMABS at different heating rates (β) (Stage II)

Where, $(1-\alpha)^2$ represent the differential form of F2 and $2(1-\alpha)^{2/3}[1-(1-\alpha)^{1/3}]^{-1}$ represent the differential form of D3. Nalini et al., have reported the 2'-amino-6'-(1Hindol-3-yl)-1-methyl-2-oxospiro-[indoline-3, 4'-pyran]-3', 5'-dicarbonitrile decomposed under F2 model [43] and Wang et al., reported a thermal decomposition kinetics of 1-(pyridinium-1-yl)-propane-(1-methyl piperidinium)bi[bis(trifluoromethanesulfonyl)imide], $[\text{PyC}_3\text{Pi}][\text{NTf}_2]_2$ under F2 model [44].

Thermodynamic parameters

The kinetic parameters, energy of activation and pre-exponential factor were obtained from Kissinger [26] single point kinetic method. Based on the values of activation energy and pre-exponential factor, the values of ΔS^\ddagger , ΔH^\ddagger and ΔG^\ddagger for the formation of activated complex [45-47] from the reactant were calculated and listed in Table 8. These values were calculated at the peak temperature T_p in the DTG curve. From the DTG curves, the peak temperatures are 590, 599 and 607 K for NMABS (Stage I) and for stage II, 824, 832, 839 at 10, 15 and 20 K/min⁻¹, respectively. These peak temperatures are used to evaluate single point kinetic parameters.

Table 8: Values of kinetic and thermodynamic parameters for the thermal decomposition of NMABS in oxygen atmosphere

Parameter	NMABS	
	Stage I	Stage II
$E_a/\text{Kj/mol}^{-1}$	111.73 ± 6.82	252.41 ± 14.47
$\ln A/A/\text{min}^{-1}$	21.80 ± 8.07	35.98 ± 9.55
$\Delta G^\ddagger/\text{kJ/mol}^{-1}$	153.32	214.39
$\Delta H^\ddagger/\text{kJ/mol}^{-1}$	106.75	245.49
$\Delta S^\ddagger/\text{J/mol}^{-1}$	-77.73	37.39
r	-0.998	-0.998

As can be seen from Table 8, the value of ΔS^\ddagger for the compound is negative value for stage I. It means that the corresponding activated complexes were with higher degree of arrangement than the initial stage [42]. The calculated E_a values coincide with invariant kinetic parameters. The positive values of ΔH^\ddagger and ΔG^\ddagger [48,49] for the compound show that they are connected with absorption of heat and non-spontaneous processes [46,47].

CONCLUSION

The compound chosen for this study decomposed into two stages. The decomposition of NMABS followed different kinetic models namely F2 for first stage and D3 for second stage, respectively. Since the activation energy values slightly varied with the conversion level, the average activation energy values were used to interpret decomposition models for each stage. The free energy changes occurred the compound that is positive values for both decomposition stages which indicate that the decomposition of studied compound is non-spontaneous process.

ACKNOWLEDGMENTS

The authors thank Head of the Department, CEESAT, Department of Energy and Environment (DEE), National Institute of Technology, Trichirapalli-620 015, Tamil Nadu, India, for recorded TGA and DTG.

REFERENCES

- [1] U.K. Singh, S.N. Pandeya, S.K. Sethia, M. Pandey, A. Singh, A. Garg, P. Kumar, *Int. J. Pharm. Sci. Drug. Res.*, **2010**, 2(3), 216-218.
- [2] A.S. Abu-Khadra, R.S. Farag, A.M. Abdel-Hady, *Am. J. Anal. Chem.*, **2016**, 7, 233-245.
- [3] V. Gomathi, R. Selvameena, *Int. J. Pharm. Pharm. Sci.*, **2014**, 6(1), 487-491.
- [4] Y.B. Zemedede, S. Ananda Kumar, *Int. J. Chem. Tech. Res.*, **2015**, 7(1), 279-286.
- [5] P. Anand, V.M. Patil, V.K. Sharma, R.L. Khosa, N. Masand, *Int. J. Drug. Des. Disc.*, **2012**, 3(3), 851-868.
- [6] S.S. Mohamed, A.R. Tamer, S.M. Bensaber, M.I. Jaeda, N.B. Ermeli, A.A. Allafi, I.A. Mrema, M. Erhuma, A. Hermann, A.M. Gbaj, *Naunyn-Schmiedeberg's Arch Pharmacol.*, **2013**, 386(9), 813-822.
- [7] Z.H. Chohan, A.U. Shaikh, M.M. Naseer, C.T. Supuran, *J. Enzyme Inhib. Med. Chem.*, **2006**, 21(6), 771-781.
- [8] Z.H. Chohan, M.H. Youssoufi, A. Jarrahpour, T.B. Hadda, *Eur. J. Med. Chem.*, **2010**, 45, 1189-1199.
- [9] S. Mondal, S.M. Mandal, T.K. Mondal, C. Sinha, *J. Mol. Struct.*, **2017**, 1127, 557-567.
- [10] S. Swamy, T. Parathasarathy, *Int. Res. J. Pharm.*, **2012**, 3(11), 213-215.
- [11] J. Anandakumaran, M.L. Sundararajan, T. Jeyakumar, M.N. Uddin, *Am. Chem. Sci. J.*, **2016**, 11(3), 1-14.
- [12] T.N. Omar, *Iraqi J. Pharm. Sci.*, **2007**, 16(2), 5-11.
- [13] R.A. Khalil, A.H. Jalil, A.Y. Abd-Alrazzak, *J. Iran. Chem. Soc.*, **2009**, 6(2), 345-352.
- [14] M.A. El-Nawawy, R.S. Farag, I.A. Sabbah, A.M. Abu-Yamin, *Inter. J. Pharm. Res. Sci.*, **2011**, 2(12), 3143-3148.
- [15] S. Kumar, M.S. Niranjana, K.C. Chaluvvaraju, C.M. Jamakhandi, D. Kadadevar, *J. Curr. Pharm. Res.*, **2010**, 01, 39-42.
- [16] E. Baher, N. Darzi, A. Morsali, S.A. Beyramabadi, *J. Korean Chem. Soc.*, **2015**, 59(6), 483-487.
- [17] N. Elangovan, T. Kolochi, S. Sowrirajan, *Int. J. Curr. Res. Chem. Pharm. Sci.*, **2016**, 3(9), 60-65.
- [18] A. Scozzafava, C.T. Supuran, *Bioorg. Med. Chem. Lett.*, **2000**, 10, 1117-1120.
- [19] M.I. Ayad, A. Mashaly, M.M. Ayad, *Thermochim. Acta.*, **1991**, 184, 173-182.
- [20] H.L. Friedman, *J. Polym. Sci. Polym. Sympos.*, **1964**, 6(1), 183-195.
- [21] J.H. Flynn, L.A. Wall, *J. Res. Natl. Bur. Stand.*, **1966**, 70(6), 487-523.
- [22] T. Ozawa, *Bull. Chem. Soc. Jpn.*, **1965**, 38(11), 1881-1886.
- [23] C.D. Doyle, *J. Appl. Polym. Sci.*, **1961**, 5(15), 285-292.
- [24] C.D. Doyle, *Nature.*, **1965**, 207, 290-291.
- [25] C.D. Doyle, *J. Appl. Polym. Sci.*, **1962**, 6(24), 639-642.
- [26] H.E. Kissinger, *Anal. Chem.*, **1957**, 29(11), 1702-1706.
- [27] T. Akahira, T. Sunose, *Res. Report (CHIBA Inst. Technol.)*, **1971**, 16, 22-31.
- [28] A.W. Coats, J.P. Redfern, *Nature.*, (London), **1964**, 201, 68-69.
- [29] H.H. Horowitz, G. Metzger, *Anal. Chem.*, **1963**, 35(10), 1464-1468.
- [30] J.M. Criado, J. Morales, *Thermochim. Acta.*, **1976**, 16(3), 382-387.
- [31] A.I. Lesnikovich, S.V. Levchik, *J. Therm. Anal.*, **1985**, 30(1), 237-262.

- [32] J.H. Flynn, *Thermochim. Acta.*, **1997**, 300(1-2), 83-92.
- [33] G.I. Senum, R.T. Yang, *J. Therm. Anal.*, **1977**, 11(3), 445-447.
- [34] H.E. Kissinger, *J. Res. Natl. Bur. Stand.*, **1956**, 57(4), 217-221.
- [35] D.J. Whelan, R.J. Spear, R.W. Read, *Thermochim. Acta.*, **1984**, 80, 149-163.
- [36] J. Málek, *Thermochim. Acta.*, **1989**, 138(2), 337-346.
- [37] H.F. Cordes, *J. Phys. Chem.*, **1968**, 72(6), 2185-2189.
- [38] C.H. Bamford, C.F.H. Tipper (Eds.), Elsevier, Amsterdam, **1980**, 22.
- [39] P. Budrugeac, *Polym. Degrad. Stab.*, **2005**, 89(2), 265-273.
- [40] S. Vyazovkin, A.I. Lesnikovich, *Thermochim. Acta.*, **1990**, 165(2), 273-280.
- [41] S. Vyazovkin, *Int. J. Chem. Kinet.*, **1996**, 28(2), 95-101.
- [42] J. Málek, *Thermochim. Acta.*, **1992**, 200, 257-269.
- [43] G. Nalini, N. Jayachandramani, R. Suresh, V. Thanikachalam, G. Manikandan, *Eur. J. Chem.*, **2016**, 7 (3), 380-386.
- [44] J. Wang, M. Wang, X. Yang, W. Zou, X. Chen, *Chin. J. Chem. Eng.*, **2015**, 23, 816-821.
- [45] J. Šesták, Academia Prague, **1984**.
- [46] D.V. Sokolskii, V.A. Druz, Vyshaya Shkola, Moscow, Russia, **1981**.
- [47] J.M. Criado, L.A. Pérez-Maqueda, P.E. Sánchez-Jiménez, *J. Therm. Anal. Calorim.*, **2005**, 82(3), 671-675.
- [48] R.Z. Hu, Q.Z. Shi, Science Press, Beijing, China, **2001**, 1st edition.
- [49] R. Hu, S. Chen, S. Gao, F. Zhao, Y. Luo, H. Gao, Q. Shi, H. Zhao, P. Yao, J. Li, *J. Hazard. Mater.*, **2005**, 117(2-3), 103-110.